Structure prediction and targeted synthesis: A new Na n N 2 diazenide crystalline structure

Xiuwen Zhang, Alex Zunger, and Giancarlo Trimarchi

Citation: The Journal of Chemical Physics **133**, 194504 (2010); doi: 10.1063/1.3488440
View online: http://dx.doi.org/10.1063/1.3488440
View Table of Contents: http://scitation.aip.org/content/aip/journal/jcp/133/19?ver=pdfcov
Published by the AIP Publishing

Structure prediction and targeted synthesis: A new Na_nN_2 diazenide crystalline structure

Xiuwen Zhang,[1] Alex Zunger,[1,a)] and Giancarlo Trimarchi[2]
[1]*National Renewable Energy Laboratory, Golden, Colorado 80401, USA*
[2]*Department of Physics and Astronomy, Northwestern University, Evanston, Illinois 60208, USA*

(Received 29 June 2010; accepted 20 August 2010; published online 19 November 2010)

Significant progress in theoretical and computational techniques for predicting stable crystal structures has recently begun to stimulate targeted synthesis of such predicted structures. Using a global space-group optimization (GSGO) approach that locates ground-state structures and stable stoichiometries from first-principles energy functionals by objectively starting from randomly selected lattice vectors and random atomic positions, we predict the first alkali diazenide compound Na_nN_2, manifesting homopolar N–N bonds. The previously predicted Na_3N structure manifests only heteropolar Na–N bonds and has positive formation enthalpy. It was calculated based on local Hartree–Fock relaxation of a fixed-structure type (Li_3P-type) found by searching an electrostatic point-ion model. Synthesis attempts of this positive ΔH compound using activated nitrogen yielded another structure (anti-ReO_3-type). The currently predicted (negative formation enthalpy) diazenide Na_2N_2 completes the series of previously known BaN_2 and SrN_2 diazenides where the metal sublattice transfers charge into the empty N_2 Π_g orbital. This points to a new class of alkali nitrides with fundamentally different bonding, i.e., homopolar rather than heteropolar bonds and, at the same time, illustrates some of the crucial subtleties and pitfalls involved in structure predictions versus planned synthesis. Attempts at synthesis of the stable Na_2N_2 predicted here will be interesting.
 [doi:10.1063/1.3488440]

I. INTRODUCTION

Laboratory synthesis and characterization of compounds are the ultimate reality tests for theoretical crystal-structure predictions. Indeed, it is not surprising that the theoretical prediction[1] and subsequent synthesis and structure determination[2–4] of a new alkali nitride Na_3N have understandably featured prominently in a recent review article on structure prediction[5] and on planned synthesis in solid-state chemistry.[6,7] Nitrides of alkali metals offer a fruitful arena for finding new crystal-structure types because of the subtlety of the competing chemical interactions. The nitrogen atom is a poor electron acceptor (having unusually low electron-affinity due to its stable half-filled p^3 shell) making it difficult to form a heteropolar M^+-N^- bond with alkali metals M; yet, the nitrogen atom has a large affinity to other nitrogen atoms with which it can form the highly stable molecular N_2. This sets up a competition between homopolar N–N and heteropolar M^+-N^- bonding within metal frameworks. Indeed, with the exception[3] of Li (forming Li_3N in the Li_3N structure having no N–N bonds), no other alkali metal was known to form any nitride from $M+N_2$ under ambient conditions. This failure of the homology principle[2]—the existence of Li_3N, but absence of Na_3N, and K_3N—stimulated the theoretical search and eventual prediction[1] of a new Na_3N crystal-structure. The predicted metastable structures[1] manifested only heteropolar M–N bonds and had *positive* formation enthalpies (ΔH) (being thus unstable with respect to metallic Na+molecular N_2). Its synthesis required the use of beams of *activated* atomic nitrogen,[2] consistent with the positive ΔH for the targeted compound.

Here, we revisit this classic problem by searching, via an evolutionary algorithm approach, for the ground states of the density-functional energy functional of the Na–N system, thus avoiding the approach of Jansen and Schön[1] of identifying candidate lowest-energy structures by searching a simple electrostatic energy functional that does not favor chemical bonding between like-charge ions (e.g., two anions). The advanced theoretical method used in this paper (i) shows improved strategies for locating stable forms of unsuspected crystal structures, thus better directing the search for new materials, (ii) explains the nature of the Na_3N compound with heteropolar Na–N bonds having $\Delta H>0$, and (iii) predicts far more stable (yet unmade) Na_2N_2 and Na_6N_2 compounds with $\Delta H<0$ in hitherto unknown structure types manifesting diatomic homopolar N–N bonds. The Na_2N_2 compound predicted here completes a missing entry in another homological series of nonalkali diazenides, $Ba^{2+}(N_2^{2-})$ and $Sr^{2+}(N_2^{2-})$, and is the first alkali diazenide. These finding point to a new class of alkali nitrides with fundamentally different bonding (homopolar molecular, rather than the heteropolar one found in Refs. 1–4) and, at the same time, illustrates some of the crucial subtleties involved in structure predictions versus planned synthesis.

a)Electronic mail: alex_zunger@nrel.gov.

SDF Optimized \ Energy Functional	Empirical Force-Field	First-Principles (HF, LDA, ...)
"Local" : • Lattice constants • Cell-internal		2
"Global" : • Lattice-type • Cell-internal	1	3

FIG. 1. Different levels of structure optimization methods based on combining various energy functionals with the type of SDFs that are optimized.

II. METHOD

A. Strategies of structure optimization

With the advent of first-principles total-energy computational methods for *periodic* solids,[8–10] two leading types of structure prediction approaches based on such calculations have developed. In the *inductive* approach (e.g., data mining,[11] or diagrammatic orbital-radii structure separation),[12] one offers a guess for the crystal structure of a given compound by analogy with known structures of other compounds, an approach that generally works very well except if one encounters a new prototype structure that is matchless (as is the case for Na–N here). In the *deductive* approach, one explicitly varies the structural degrees of freedom (SDFs) of a (say, A_pB_q) compound in search of a minimum of a given energy functional. The latter can be either a "first-principles" functional based on a microscopic Hamiltonian with explicit electronic coordinates (e.g., Hartree–Fock; density-functional), or an empirical "force field," in which the electronic coordinates are integrated out and one focuses on a subset of the chemical interactions deemed important (e.g., a point-ion electrostatic potential with some repulsive walls is used).[1]

The selection of the SDF being optimized divides the energy minimization methods into different optimization classes illustrated in Fig. 1. (i) In one common approach one fixes at the outset the type of unit cell lattice vectors (e.g., orthorhombic or monoclinic) and the occupancy of the space-group specific (Wyckoff) atomic sites, (e.g., NaCl versus fluorite site occupation of the $Fm\bar{3}m$ space-group) and optimize the remaining SDFs, i.e., the magnitude of the lattice parameters and cell-internal parameters not decided by symmetry. Such "local optimization"[13–15] (Fig. 1) is ubiquitous and has been implemented in most standard solid-state total-energy packaged codes.[10,16] This approach requires *a priori* knowledge of the structure type appropriate for a given compound and thus affords but a limited "surprise factor" in identifying unsuspected structures. (ii) In the "global space-group optimization" approach one starts from randomly selected lattice vectors and random Wyckoff positions and uses global optimization and search methods, (e.g., evolutionary algorithm[17] and simulated annealing)[18] to zoom-in in an unbiased manner to the minimum energy. Unlike the local relaxation (a positional optimization), in the global crystal-structure search (both a positional and configurational optimization) A and B atoms can swap positions during the calculation and the lattice-type can change (e.g., bcc to fcc) in search of lower energy topologies. In a recent development,[19] such approaches were generalized to optimize the stable stoichiometries (p,q) in A_pB_q "on the fly." The different combinations of energy functionals with either local or global structure optimization (Fig. 1) define the various classes (1, 2, or 3) of deductive structure predictions. As we will see below the selection of such a class can critically control the qualitative and quantitative outcome of the structure prediction.

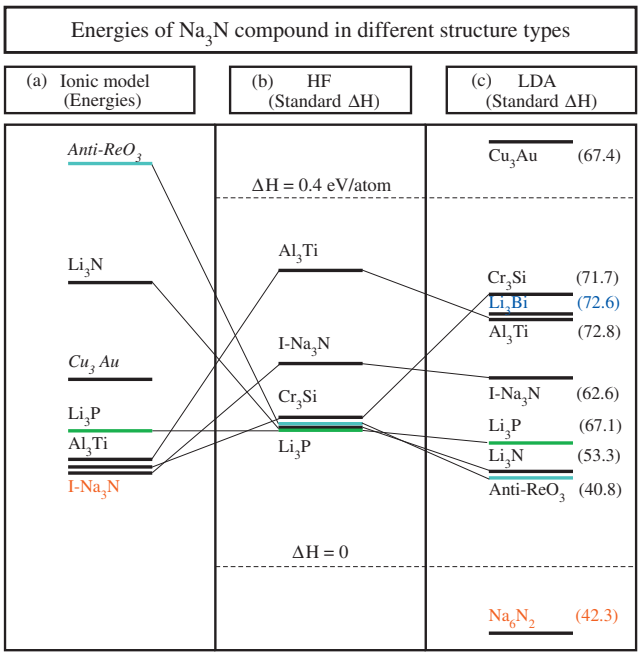

FIG. 2. Calculated energies of Na_3N in different structure types: (a) energies obtained in the empirical ionic model (taken from Table III of Ref. 1 and Fig. 6 of Ref. 2), (b) Hartree–Fock standard formation enthalpies from local optimization (taken from Table III of Ref. 1 and Fig. 2 of Ref. 2), and (c) LDA standard formation enthalpies (present study). The density of each structure type in LDA is given in (c) in parentheses (in atom/nm^3). Entries in red were obtained from global optimization. The energy of the Li_3P structure type given by the ionic model in (a) was arbitrarily aligned with its corresponding HF standard formation enthalpy in (b).

B. Search for heteropolar Na–N structures

Jansen and Schön[1] (see also reviews in Refs. 5–7) used an empirical point-ion electrostatic force field in conjunction with a global optimization technique (method 1 in Fig. 1) identifying candidate structures for Na_3N, with energies shown in Fig. 2(a). Since an electrostatic point-ion energy functional can not stabilize like-charge (homopolar) bonds, all structures found (shown in Fig. 3) exhibited only heteropolar Na–N contacts. The lowest-energy structure was a previously unknown structure type denoted I–Na_3N [in Fig. 2 and shown in Fig. 3(e)].

These candidate structures obtained by the empirical functional were then subjected to a *local* optimization, using a first-principles Hartree–Fock (HF) energy functional (method 2 in Fig. 1). Having accepted the fixed-structure types (from the electrostatic functional), the local optimization procedure cannot create new structures other than those

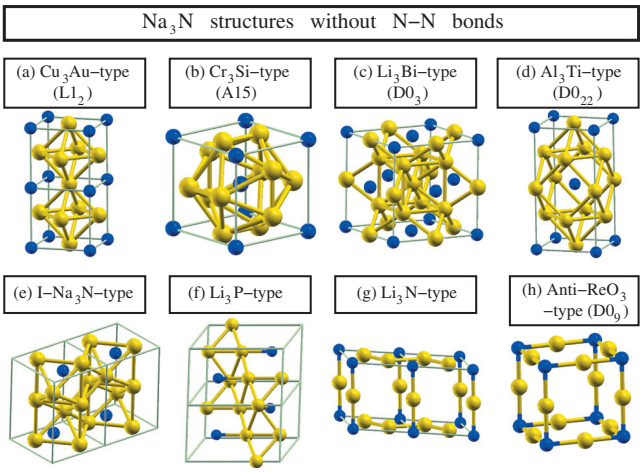

FIG. 3. Candidate structure types of Na_3N that lack N–N bonds that were considered in the literature. Large yellow spheres: Na. Small blue spheres: N. LDA ΔH values are (a) 0.461, (b) 0.292, (c) 0.272, (d) 0.272, (e) 0.205, (f) 0.134, (g) 0.103, and (h) 0.096, all in eV/atom.

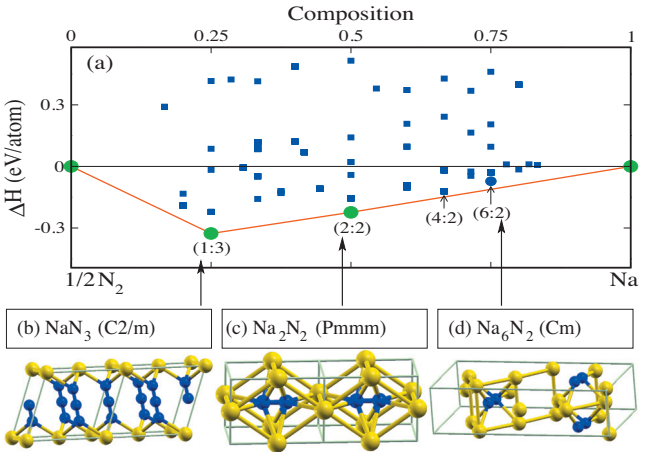

FIG. 4. (a) Evolution of the calculated formation enthalpies of the structures of Na–N system visited during the global space-group optimization using the LDA energy functional (squares). [(b)–(d)] The structures found. Large yellow spheres: Na. Small blue spheres: N.

fed to it. The ensuing HF formation enthalpies are shown in Fig. 2(b). The lowest-energy structure of Na_3N is now the Li_3P structure type. Notably, the order of stability is very different in Fig. 2(a) (electrostatics) and Fig. 2(b) (Hartree–Fock) [e.g., see the energy order of the Al_3Ti and Li_3N structure types in (a) versus (b)], reflecting the limited ability of the simple point-ion electrostatic force field to describe chemistry. Given the positive formation enthalpies of all heteropolar structures predicted in Fig. 2(b) with respect to metallic Na and free-space N_2, subsequent synthesis[2–4] proceeded using excited forms of "active nitrogen." The structure found in synthesis[2–4] was the anti-ReO_3-type ($D0_9$). (This is not the lowest-energy structure in the electrostatic model [Fig. 2(a)] or the HF model [Fig. 2(b)].) Our own local optimization using the local density approximation (LDA) energy functional[20] [Fig. 2(c)] resolves the latter conflict, giving the observed[2–4] anti-ReO_3 structure type as the lowest-energy structure for Na_3N under the same restriction to heteropolar bonds.

Fischer *et al.*[21] suggested that in their synthesis method, the route to the final compound went via the amorphous stage, which typically has the lowest atomic density. Figure 2(c) gives (in parentheses) the calculated atomic densities (in atom/nm^3) of all heteropolar phases. Indeed, the observed anti-ReO_3 structure type of Na_3N has the lowest atomic density. Jansen and Schön[1] predicted from electrostatics that the three lowest-energy structure types were I–Na_3N, Cr_3Si, and Al_3Ti. Then, Hartree—Fock calculations[1] gave Li_3P, Li_3N, and anti-ReO_3 as the three lowest-energy structure types for Na_3N. Their synthesis[2] gave anti-ReO_3 structure type. Here, we point to the possible pitfall of not consistently using a high-accuracy energy functional (for instance LDA), in a global search of the lowest-energy structure instead of following a two-step scheme—using a model functional to select a handful of candidate lowest-energy structures and then locally relaxing it at the quantum mechanical level. Not only does the latter prescription suffer from the approximate nature of the model energy functional, but it is also prone to the arbitrariness of the choice of how many of the lowest-energy structures found via empirical functional to calculate with an *ab initio* method. In this sense, the fact that Jansen and Schön calculated Li_3P-type, Li_3N-type, or anti-ReO_3 structures with HF should be regarded as accidental as no indication was given by electrostatics that these crystal structures predicted by this model to be rather high-energy ones would be the three of lowest energy in HF.

C. Present method

Given the limitations of the previous methodology—*global* optimization with an electrostatic functional, followed by *local* refinement of the structures with a self-consistent functional—we sought to find the structure types and compositions of Na–N compounds without these restrictions. We use the composition (x)-dependent global space-group optimization (Ref. 19) within the LDA to the density-functional theory (method 3 in Fig. 1). In this approach, the structure type is not prejudged as we start from randomly selected lattice vectors and randomly selected Wyckoff positions. We use[19] a real-space genetic algorithm ("cut and splice")[22] as applied to periodic structures.[23] We search for "ground-state structures," i.e., for the breaking point of the convex hull of energy versus composition. The application of this search scheme to the Na–N system also allows us to emphasize the general procedure to correctly predict the stable phases of a binary system.

III. RESULTS AND DISCUSSION

A. Finding alkali structures with embedded homopolar N_2

Figure 4(a) shows the evolution of the calculated standard formation enthalpies of the structures of Na–N system visited during the global space-group optimization[24] (squares). The red line is the convex hull, which connects the lowest-energy configurations at the compositions (solid circles) that are simultaneously stable with respect to disproportionation into two configurations at neighboring compo-

sitions. Significantly, none of the heteropolar Na–N structures discussed before[1,2,6] emerged here as ground-state structures. Instead, we find numerous structures with negative ΔH at different compositions, including two ordered structures at compositions 1:3 and 2:2 on the convex hull, i.e., ground-state structures.

The NaN_3 ground-state structure we find [1:3 in Fig. 4(a), see also Fig. 4(b)] is the well-known sodium azide structure,[25] which is monoclinic with space-group $C2/m$, has calculated lattice parameters of $a=5.91$ Å, $b=3.31$ Å, $c=5.06$ Å, $\beta=108.3°$, and has eight atoms in the unit cell at Wyckoff positions of Na $2a(0,0,0)$, N $2d(0,1/2,1/2)$, and N $4i(0.10,1/2,0.74)$. The N–N bond length in this structure is 1.17 Å, in agreement with the experimental result.[25]

The Na_2N_2 ground-state structure we find [2:2 in Fig. 4(a)] is a new structure type (we confirm by searching all prototypes in Pearsons Handbook of Crystallographic Data for Intermetallic Phases[26] that the prototype found here has not been previously reported), which has LDA formation enthalpy of −0.223 eV/atom (−86 kJ/mol of Na_2N_2), and in generalized gradient approximation (GGA) has a slightly positive ΔH of 4 kJ/mol.[27] The depth of ΔH of Na_2N_2 on the convex hull with respect to the tie-line between NaN_3 and Na is ~5 meV/atom, which is within the relative convergence error of points on the convex hull. Its structure [Fig. 4(c)] is orthorhombic with space-group *Pmmm*, calculated lattice parameters of $a=3.04$ Å, $b=3.58$ Å, $c=4.99$ Å, and four atoms in the unit cell at Wyckoff positions Na $1c(0,0,1/2)$, Na $1e(0,1/2,0)$, and N $2t(1/2,1/2,0.38)$. The LDA N–N bond length in this structure is 1.24 Å. The N_2 molecules sit inside Na_8 parallelepipeds. On the plane perpendicular to the N_2 molecule, there are four Na atoms each connecting to both N atoms. At each end of the N_2 molecule, there are two Na atoms connecting to the N atom. There are chains of face-sharing parallelepipeds, which also share edges in the directions perpendicular to the chain.

The Na_6N_2 structure we find [6:2 composition in Fig. 4(a)] has LDA formation enthalpy of −0.072 eV/atom (−56 kJ/mol). In GGA, its ΔH is positive 21 kJ/mol (for comparison, GGA predicts a far more positive ΔH of 85 kJ/mol for the anti-ReO_3-type Na_3N, which was measured[3] to be 64 kJ/mol). Na_6N_2 lies ~40 meV/atom above the convex hull, but it is considerably more stable than all the structures without N–N bonds (see Fig. 2). Its structure [Fig. 4(d)] is monoclinic with space-group *Cm*, calculated lattice parameters of $a=13.55$ Å, $b=3.24$ Å, $c=8.79$ Å, $\beta=101.4°$, and 16 atoms in the unit cell at Wyckoff positions Na $2a(0.58,0,0.58)$, Na $2a(0.84,0,0.57)$, Na $2a(0.42,0,0.23)$, Na $2a(0.17,0,0.28)$, Na $2a(0.76,0,0.90)$, Na $2a(0.02,0,0.92)$, N $2a(0.21,0,0.54)$, and N $2a(0.23,0,0.68)$. The LDA N–N bond length of molecular N_2 in this structure is 1.22 Å. In this structure, the N_2 molecule is surrounded by seven Na atoms, forming face-sharing triangular prisms and pyramids.

The Na_nN_2 structures we find differ from the BaN_2 and SrN_2 diazenide structures. In BaN_2 (Ref. 28) and SrN_2,[29] the metallic atoms (Ba or Sr) form a distorted bcc sublattice, and the N_2 molecules occupy the octahedral interstitial sites with orientations along two (for BaN_2) or one (for SrN_2) diagonals of the M_6 octahedra. In the structures of Na_2N_2 [Fig. 4(c)] and Na_6N_2 [Fig. 4(d)], the Na sublattices are quite different from bcc, and the N_2 molecules are surrounded by Na_8 parallelepipeds (for Na_2N_2) or Na_7 polyhedra (for Na_6N_2). The LDA-calculated N–N bond lengths in Na_2N_2 and Na_6N_2 are both close to the observed N–N bond lengths in BaN_2 (1.22 Å) (Ref. 28) and SrN_2 (1.22 Å) (Ref. 29) diazenides. The Na_6N_2 is a subdiazenide having excess metal atoms similar to the suboxide materials.[30] We also find a few other sodium subdiazenides [Na_nN_2 with $n>2$], e.g., Na_4N_2, which lies ~28 meV/atom above the convex hull [see Fig. 4(a)].

B. Electronic structure

We show in Fig. 5 the calculated density of states (DOS), including assignment of various peaks from a separate analysis of the local DOS and the energy-integrated DOS (not shown here). Recall that the ten-valence-electron N_2 free molecule has the molecular orbitals $1\Sigma_g^2(2s)2\Sigma_u^2(2s)1\Pi_u^4(2p)3\Sigma_g^2(2p)2\Pi_g^0(2p)$, where the superscripts denote the orbital occupancy and the parentheses give the atomic orbital parentage. We find from Fig. 5 that both Na_2N_2 and Na_6N_2 have fully occupied Na $2p^6$, as well as dinitrogen $[1\Sigma_g^2(2s)2\Sigma_u^2(2s)1\Pi_u^4(2p)3\Sigma_g^2(2p)]$ like states. In contrast with the free-space N_2 molecule having an empty $2\Pi_g(2p)$ state, in the Na_2N_2 and Na_6N_2 solids the nitrogen diatomic units receive additional charge within states located ≤2 eV below the Fermi level (E_F) in Fig. 5. These are mainly the $2\Pi_g(2p)$ states of dinitrogen in Na_2N_2 and a mixture of $2\Pi_g(2p)+(\mathrm{Na},3s)+$other states in Na_6N_2. This addi-

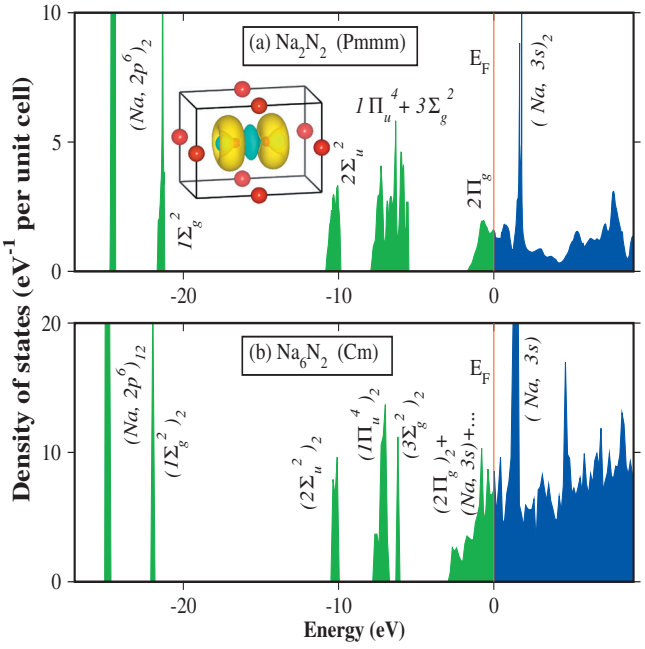

FIG. 5. Total densities of states from LDA calculations of (a) Na_2N_2 and (b) Na_6N_2. Peaks are approximately identified by their orbital character and occupancy (superscript). Inset: charge density difference (isosurfaces ±0.035 e/Å^3, positive value in yellow, and negative value in blue) with respect to atomic Na and isolated molecular N_2 with the bond length in Na_2N_2. The position of Na (N) atom is indicated by the large (small) red sphere. There is a sea of small (not shown by the isosurfaces) negative charge density difference surrounding Na atoms.

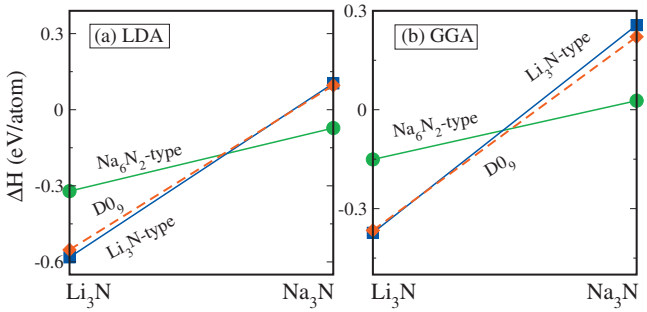

FIG. 6. Formation enthalpies of M_3N (M=Li,Na) compounds (shown on abscissa) in either the Na_6N_2-type structure (that have N–N bonds) and the anti-ReO_3-type ($D0_9$) and Li_3N-type structures (that lack N–N bonds) from LDA and GGA calculations.

tional charge elongates the N–N bond (the N–N bond length of the free-space N_2 molecule is 1.10 Å in LDA). The main part of the Na 3*s* state is above E_F (i.e., empty). The $2\Pi_g(2p)$ state consists of the p_x, p_y states of dinitrogen and looks like two toruses surrounding the two N atoms. The additional charge filling the $2\Pi_g(2p)$ state is distributed in these two toruses [see the inset figure of Fig. 5(a)]. This electronic structure is similar to that of BaN_2 (Ref. 28) and SrN_2 (Ref. 29) diazenides. We have estimated the charge transfer from the metal sublattice to the nitrogen diatomic units by integrating the difference between the charge density of the solid minus the charge densities of the M atoms and N_2 molecules at the respective positions in the solid [inset to Fig. 5(a)], finding Q=0.60e for Na_2N_2; Q=0.79e for Na_6N_2 compared with Q=0.51e in SrN_2. These values are smaller than the idealized Q=2e value assigned classically.

C. M–N versus M–N_2 structures

Are the molecular structures [e.g., Fig. 4(d)] always more stable than the nonmolecular ones (e.g., Fig. 3)? To answer this question, we show in Fig. 6 the calculated formation enthalpies of the Na_3N and Li_3N compounds both in the Na_6N_2 (*Cm*) structure [see Fig. 4(d)] and in the atomic anti-ReO_3 and Li_3N-type structures. We see that whereas in the Na_3N compound the molecular phase is more stable (both in LDA and GGA), in the Li_3N compound the atomic phases are more stable (both in LDA and GGA). This agrees with experimental phase diagram[31] of Li_3N.

D. Lithium-nitrogen system

The Li_3N (Ref. 31) and LiN_3 (Ref. 25) are the two known phases in the Li–N system. We calculate the formation enthalpy of Li_2N_2 in the Na_2N_2 (*Pmmm*) structure [see Fig. 4(c)] finding −0.644 eV/atom in LDA and −0.345 eV/atom in GGA. The calculated formation enthalpy of Li_3N in the Li_3N-type structure is measured[32] to be −0.409 eV/atom, and calculated to be −0.582 eV/atom in LDA and −0.373 eV/atom in GGA. The calculated ΔH of LiN_3 in the lithium azide structure[25] is −0.436 eV/atom in LDA and −0.146 eV/atom in GGA. Thus, we predict Li_2N_2 to have negative ΔH, lower than the tie-line between Li_3N and LiN_3. Thus, it is stable against disproportionation into Li_3N and LiN_3. In Ref. 31, only the Li–Li_3N part of the lithium-nitrogen phase diagram was measured. Thus, attempts at synthesis of Li_2N_2 will be interesting. The lithium-nitrogen system is similar to the barium-nitrogen system, which has the stable nonmolecular phase Ba_3N_2 and molecular phase BaN_2.[28]

IV. CONCLUSIONS

Using global structure optimization within a first-principles energy functional combined with the calculation of the convex hull that identifies the stable stoichiometries, we predict the first diazenide of an alkali metal. The structure of this compound consists of N_2 molecules inside Na_8 parallelepipeds, the latter forming chains that share edges. The stability of this structure stems from the transfer of the electrons previously occupying Na 3*s* orbital to the previously empty $2\Pi_g(2p)$ orbital of N_2. The previously predicted Na_3N structures without such N–N bonds represent metastable local minima appearing in synthesis that favors low-atomic-density networks.

ACKNOWLEDGMENTS

We thank Professor Martin Jansen for correspondence of his works (Refs. 1, 2, and 6) and for pointing out to us Ref. 29. We are grateful to Professor Kenneth R. Poeppelmeier and Dr. Stephan Lany for very helpful discussions. This research was supported by the U.S. Department of Energy, Office of Basic Energy Sciences, Division of Materials Sciences and Engineering, Energy Frontier Research Centers, under Award No. DE-AC36-08GO28308 to NREL.

[1] M. Jansen and J. C. Schön, Z. Anorg. Allg. Chem. **624**, 533 (1998).
[2] D. Fischer and M. Jansen, Angew. Chem., Int. Ed. **41**, 1755 (2002).
[3] G. V. Vajenine, Inorg. Chem. **46**, 5146 (2007).
[4] G. V. Vajenine, Solid State Sci. **10**, 450 (2008).
[5] S. M. Woodley and R. Catlow, Nature Mater. **7**, 937 (2008).
[6] M. Jansen, Angew. Chem., Int. Ed. **41**, 3746 (2002).
[7] K. D. M. Harris and P. P. Edwards, *Turning Points in Solid-State, Materials and Surface Science* (RSC Publishing, Cambridge, UK, 2007).
[8] E. Wigner and F. Seitz, Phys. Rev. **43**, 804 (1933).
[9] J. Ihm, A. Zunger, and M. L. Cohen, J. Phys. C **12**, 4409 (1979).
[10] S. Wei, H. Krakauer, and M. Weinert, Phys. Rev. B **32**, 7792 (1985).
[11] S. Curtarolo, D. Morgan, K. Persson, J. Rodgers, and G. Ceder, Phys. Rev. Lett. **91**, 135503 (2003).
[12] A. Zunger and M. L. Cohen, Phys. Rev. Lett. **41**, 53 (1978).
[13] M. T. Yin and M. L. Cohen, Phys. Rev. B **26**, 5668 (1982).
[14] S. Froyen and M. L. Cohen, Phys. Rev. B **28**, 3258 (1983).
[15] J. Hafner, C. Wolverton, and G. Ceder, MRS Bull. **31**, 659 (2006).
[16] G. Kresse and J. Furthmůller, Comput. Mater. Sci. **6**, 15 (1996).
[17] D. A. Coley, *An Introduction to Genetic Algorithms for Scientists and Engineers* (World Scientific, Singapore, 1999).
[18] S. Kirkpatrick, J. Stat. Phys. **34**, 975 (1984).
[19] G. Trimarchi, A. J. Freeman, and A. Zunger, Phys. Rev. B **80**, 092101 (2009).
[20] Total energies were calculated from density-functional theory, using a plane-wave basis set. We used the augmented-wave pseudopotentials, and the LDA exchange-correlation functional of Perdew and Zunger (Ref. 33) (or the Perdew–Burke–Ernzerhof exchange-correlation functional) (Ref. 34). Basis set energy-cutoff was set to be 500 eV. The reciprocal space was sampled using grids with densities of $2\pi\times0.051$ and $2\pi\times0.034$ Å^{-1} for relaxation and static calculation, respectively. Overall convergence of total energy is ~5 meV/atom.
[21] D. Fischer, Ž. Čančarevič, J. C. Schön, and M. Jansen, Selected research reports: First synthesis of Na_3N based on rational synthesis planning concepts.
[22] D. M. Deaven and K. M. Ho, Phys. Rev. Lett. **75**, 288 (1995).

[23] A. R. Oganov and C. W. Glass, J. Chem. Phys. **124**, 244704 (2006).
[24] The structure search was performed for structures with up to 20 atoms per unit cell. The population size was set to 16 and the two worst individuals were replaced by offspring at each generation. The rate of crossover versus mutation was set to 0.7. A minimum of two independent evolutionary runs with 30 or more generations were performed for each global space-group optimization search.
[25] W. Zhu, J. Xiao, and H. Xiao, J. Phys. Chem. B **110**, 9856 (2006).
[26] P. Villard and L. D. Calvert, *Pearson's Handbook of Crystallographic Data for Intermetallic Phases* (ASM International, Materials Park, OH, 1991).
[27] We are uncertain about the ability of LDA/GGA to produce accurate absolute ΔH values because of LDA/GGA errors (e.g., the calculated ΔH of BaN_2 is −250 kJ/mol in LDA and −152 kJ/mol in GGA, and was measured to be −172 kJ/mol) (Ref. 32), but the structure search was guided well by LDA.
[28] G. V. Vajenine, G. Auffermann, Y. Prots, W. Schnelle, R. K. Kremer, A. Simon, and R. Kniep, Inorg. Chem. **40**, 4866 (2001).
[29] G. Auffermann, Y. Prots, and R. Kniep, Angew. Chem., Int. Ed. **40**, 547 (2001).
[30] A. Simon, Z. Anorg. Allg. Chem. **395**, 301 (1973).
[31] T. B. Massalski, J. L. Murray, L. H. Bennett, and H. Baker, *Binary Alloy Phase Diagrams* (American Society for Metals, Metals Park, OH, 1986).
[32] D. D. Wagman, W. H. Evans, V. B. Parker, R. H. Schumm, I. Halow, S. M. Bailey, K. L. Churney, and R. L. Nuttall, J. Phys. Chem. Ref. Data Suppl. **11**, 284, 285, and 295 (1982).
[33] J. P. Perdew and A. Zunger, Phys. Rev. B **23**, 5048 (1981).
[34] J. P. Perdew, K. Burke, and M. Ernzerhof, Phys. Rev. Lett. **77**, 3865 (1996).